Chinese Science Bulletin

Interaction between adjacent left-lateral strike-slip faults and thrust faults: the 1976 Songpan earthquake sequence

YUE Han, ZHANG ZhuQi & Y. John CHEN†

Department of Geophysics, School of Earth and Space Sciences, Peking University, Beijing 100871, China

Based on the published focal mechanisms we have built the fault model of the main shocks of the 1976 Songpan earthquake sequence and calculated the coseismic Coulomb stress changes in the region. The results show that most of the aftershocks had occurred in the region where the Coulomb stresses had been increased, indicating a triggering relationship between the main shocks and the aftershocks. We also show that the first main shock (M_s = 7.2), which is a left-lateral slip event, had increased the Coulomb stresses by 5×10^5 Pa at the second main shock (a thrust event with M_s = 6.7). Therefore, we conclude that the first main shock had triggered the second main shock. The third main shock is also a left-lateral event, however, the triggering relationship between the third main shock and the previous two events is less obvious. General model calculations show that there is a good triggering relationship between adjacent left-lateral slip fault and thrust fault, but triggering between parallel slip faults is rather weak.

Songpan earthquake sequence, Coulomb stress change, left-lateral slip fault, thrust fault

The Songpan earthquake sequence consists of three main shocks, which occurred in the Huya fault between Sonpan and Pingwu in the north of Sichuan Province in 1976. The first main shock struck at 22:06 on August 16 with a magnitude of 7.2, which was followed by another two events 6 and 7 days later, at 22:05 on August 22 and 11:30 on August 23 with magnitude of 6.7 and 7.2, respectively.

1 Regional geology

The 1976 Songpan earthquake sequence occurred at the east edge of the Tibetan Plateau. The eastward extrusion of the Tibetan crust resulting from the Indian-Asia continental collision is blocked here by the Ordos block in the north and the Sichuan basin in the south and as a consequence, it caused active local deformation at various fault structures here (Figure 1). Located at the north of Songpan earthquake sequence is the Kunlun strike-slip Fault[2], and at the south-east is the Longmenshan thrust fault. Altogether this is one major earthquake zone in Sichuan Province where many large earthquakes have occurred: the Diexi earthquake (M = 7.5) on August 25, 1933, the Dayixi earthquake (M = 6.2) at the south part of Longmenshan thrust fault on February 24 ,1970. From May 1973 to the end of 1974 four earthquakes with a magnitude greater than 5 had occurred between Songpan and Nanping and the largest magnitude was 6.2.

The Huya fault on which the Songpan earthquake occurred is located in the triangle zone between the Kunlun fault and the Longmenshan thrust fault[1,2]. The Huya fault has been considered as part of the Kunlun fault system and together with the Minjiang fault to its west, both form the boundary of the Minshan block[1,2]. The dominant deformation of the Minshan block is its southward motion relative to the Sichuan basin, which is

Received May 25, 2007; accepted February 4, 2008
doi: 10.1007/s11434-008-0210-z
†Corresponding author (email: johnyc@pku.edu.cn)

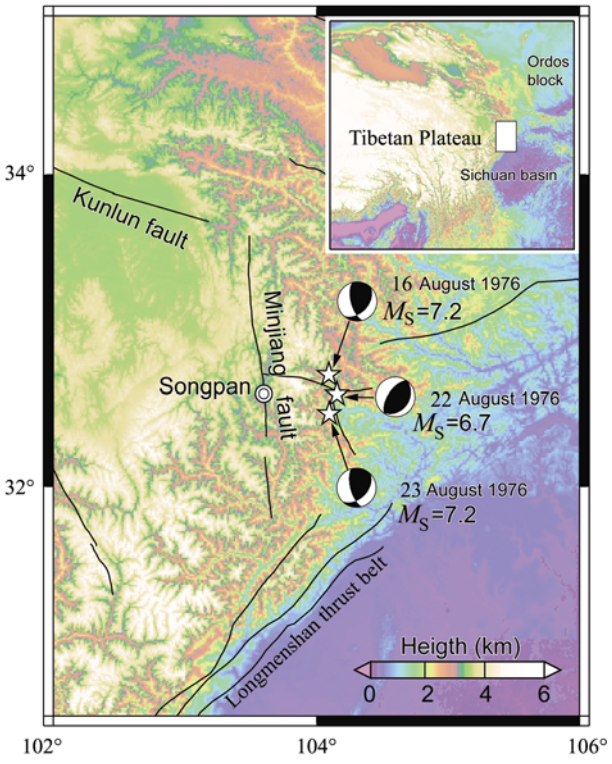

Figure 1 Regional geology of the 1976 Songpan earthquake sequence. The white rectangle is the focal region of the earthquake and the white pentacles are the position of the three main shocks of the sequence.

consistent with the focal mechanism of the Songpan earthquake sequence. The three main shocks of the sequence have struck three locations along the Huya fault[1,2] (Figure 1). The north segment and south segment are parallel to each other with a strike of 165°. The middle segment has a strike of 215° and the three segments make up a step system (Figure 2).

The Xianshuihe fault is located about 300 km southwest of the Songpan earthquake sequence and it is part of the left-lateral slip fault system at the east boundary of Tibetan Plateau. The 1973 Luhuo earthquake (M_s = 7.6) occurred at this fault[4,5]. To its west is another left-lateral slip fault, the Yushu-Garzê fault. A pull-apart basin was formed between these two faults, where many aftershocks $M_s \geqslant 3.0$ took place with the largest aftershock (M_s = 6.8) of Luhuo earthquake at a normal fault striking northeast. Liu et al.[5] have calculated the coseismic Coulomb stress changes of the 1973 Luhuo earthquake at these northeast striking normal faults Their results show that these aftershocks indeed occurred in the region where Coulomb stresses were significantly increased, indicating a good triggering relationship between the main shock and these aftershocks.

The 1976 Songpan earthquake sequence is not very far (~300 km) from the 1973 Luhuo earthquake, and both events have some similarities, such as that they both occurred on left-lateral strike-slip faults and small dipping faults exist between these strike-slip faults. During the 1976 Songpan earthquake sequence, the second event occurred on a thrust fault which is followed by another left-lateral strike-slip the next day[6]. We also notice that 7 months after the main shock of the 1973 Luhuo earthquake another left-lateral strike-slip earthquake (M_s = 5.8) also occurred on the Yushu-Garzê fault[6]. Besides the difference in the magnitude, the 1976 Songpan earthquake sequence and the 1973 Luhuo earthquake sequence share a similar pattern of left-lateral, thrust, and left-lateral strike-slip events, and the left-lateral strike-slip faults are close to parallel. By computing the Coulomb stress changes of the 1976 Songpan earthquake sequence in this study, we found that this kind of earthquake sequence could be the con-

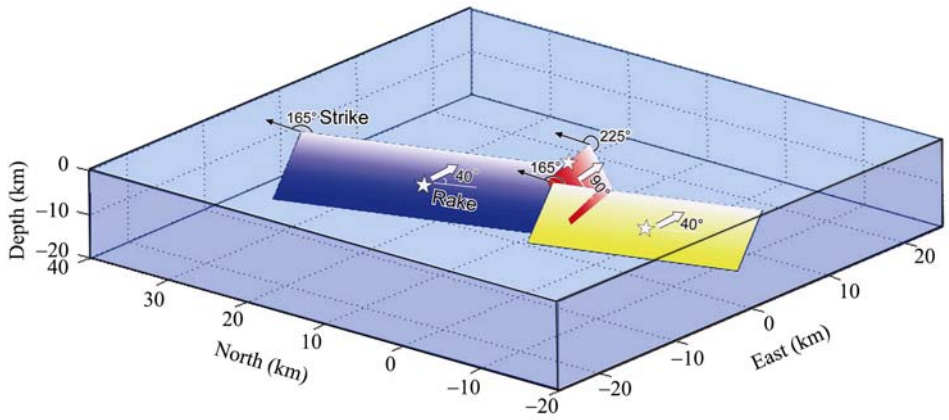

Figure 2 Fault model for Coulomb stress computing.

sequence of stress triggering between adjacent faults and it may provide new insights of understanding the earthquake distribution in this region.

2 Data and method

The source parameters of Songpan earthquake sequence (Table 1) we used in this study are from the published work of Jones et al.[6], which were derived from both the relocation and wave form modeling methods.

Table 1 Parameters of the three main shocks of Songpan earthquake sequence

	August 16	August 22	August 23
Magnitude (M_S)	7.2	6.7	7.2
Latitude (°)	32.72	32.61	32.48
Longitude (°)	104.09	104.15	104.10
Length (km)	30	12	22
Width (km)	12	8	11
Strike (°)	165	215	165
Rake (°)	40	90	40
Depth (km)	12	5	8
Moment (10^{18} Nm)	13.0	4.0	8.4
Dip (°)	63	60	65
Slip (m)	1.1	1.2	1.1

We assume a rectangle faulting surface for each major event. Since the rupture propagates in both directions for the first and third main events, we assume that the hypocenter is in the center of the rectangle. While, the rupture propagates in one direction for the second event, we assume that the hypocenter is on the north edge of the rectangle. Figure 2 shows that the three faults make a step form.

The fault model uses the parameters from Jones[6]. White arrow incdicates the rake and the black arrow indicates the north. Pentacle marks the hypocenter. The first and third main shocks occurred at the center of the fault and the second event occurred on the northern edge of the fault. Different faults are marked by different colors with the upper edge marked as white.

Cheng et al.[7] had obtained the principal axis directions by the unique station method. Their result showed that most of the stations were associated with a horizontal principal axis trending east-west, while the Songpan station, which is close to the fault, was associated with a horizontal principal axis trending north-south which is almost perpendicular to the others. On the other hand, Diao et al.[8] had also reported that most of the small earthquakes have a horizontal principal axis trending east-west. These previous work had all shown that the principal axis of this region trended east-west, except the observation at the Songpan station. Since the Songpan station is almost at the Minjiang fault, the observed result at this station may be strongly influenced by the fault geometry and could be different from the regional stress field. Thus we used the east-west horizontal principal axis in formulating our model for the computation that follows (Table 2).

Table 2 Stress field in the local region

P axis		*N* axis		*T* axis	
Direction	Dip	Direction	Dip	Direction	Dip
112°	3°	101°	78°	33°	11°

We assumed the Poisson's ratio of the rock was 0.164, which was used by Jones et al.[6] in the wave form modeling. We used the Yang's modulus for a sandstone (7942 MPa) in our model. In the calculation of the Coulomb stress, the effective friction coefficient includes the effect of both the pore pressure and the rock friction coefficient. Generally, a value for the effective friction coefficient from 0.4 to 0.8 is reasonable, so we assumed the effective friction coefficient to be 0.4.

By the Okada fault displacement model on an elastic half space[9], we can calculate the coseismic stress induced by the fault slip. When we restrain the stress to a given fault plain (the receiving fault), we can obtain the normal stress change $\Delta\sigma_n$ (a compress stress is assumed to be positive) and shear stress change $\Delta\tau_s$ on the fault surface. Then using the equation of $\Delta\sigma_c = \Delta\tau_s - \mu'\Delta\sigma_n$ we can get the Coulomb stress change on the receiving fault. Generally speaking, an increase in the Coulomb stress would increase the chance of triggering an earthquake, while, a decrease in the Coulomb stress would delay or restrain the occurrence of an earthquake[10,11].

3 Results

3.1 Aftershocks triggering

In principle the regional stress field can be perturbed by the stress change of a major event. Assuming small faults trend in all directions, the orientation of the optimal rupture plane depends on the orientation of the principal axes according to the Coulomb failure criterion. Since aftershocks are in general small in magnitude (usually without a known focal mechanism), it is usually assumed that an aftershock should occur on the optimal rupture plane at a given location. By comparing the af-

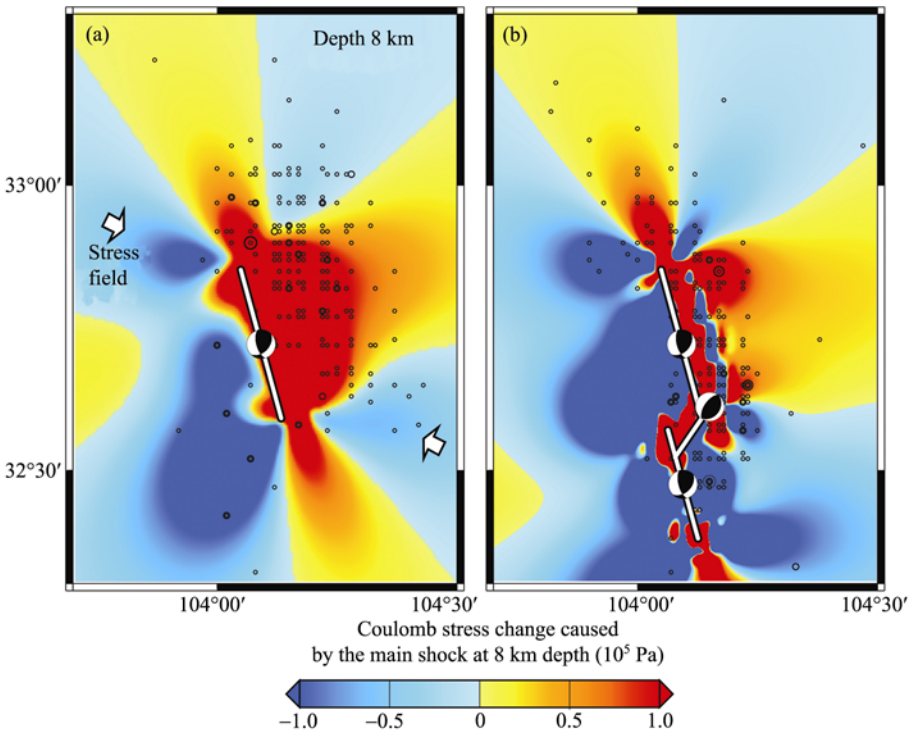

Figure 3 Coulomb stress change caused by the main shocks and the location of the after shocks. (a) Coulomb stress change on the optimal fault caused by the first main shock and the distribution of the aftershocks occurred between the first and second main shocks. Most of the aftershocks were in the region where Coulomb stress was increased. (b) Coulomb stress change on the optimal fault caused by the three main shocks and the distribution of the aftershocks occurred in the three-month period after the third main shock. Most of the aftershocks occurred in the narrow region where Coulomb stress was increased.

tershock distribution with the area of increasing Coulomb stress on the optimal rupture planes, we can investigate the triggering effect of the aftershocks.

The Coulomb stress change caused by the first main shock was compared with the locations of the aftershocks occurring before the second event (Figure 3(a)). Because the third main shock occurred only one day after the second one, there were few aftershocks between these two main shocks. Figure 3(b) shows the net Coulomb stress change caused by all these three main shocks and the location of the aftershocks occurring in the three-month period after the third main shock. It is clear from Figure 3 that most of the aftershocks fall in the region of an increase in the Coulomb stress, which indicates a strong triggering effect of these aftershocks by these main shocks of the 1976 Songpan earthquake sequence.

3.2 Triggering relationship between mainshocks

We next investigate the triggering effects among these main events of the 1976 Songpan earthquake sequence. Our calculations (Figure 4) show that the first main shock has increased the Coulomb stress at the location of the second main shock. To minimize the edge effect of the rupturing surface, we used 5 concentric rectangles to fit the unique rectangle fault plane. For a given seismic moment, we set different displacements for the five concentric rectangles and these displacements are decreased from center to zero at the edge. The Coulomb stress change on a horizontal plane at the 5-km depth is shown in Figure 4(a), and the Coulomb stress change is also shown in Figure 4(b) along the fault plane of the second main shock. The first main shock has increased the Coulomb stress by 5×10^5 Pa at the location of the second event, and therefore, it is likely that the second main event (6 days later) could be triggered by the first main shock.

By calculating the Coulomb stress changes at the location of the third main shock, Figure 5 shows that while the first main shock had decreased the Coulomb stress at this location by about $(0.3-0.4)\times10^5$ Pa, the second main shock has increased the Coulomb stress at this location by about 0.5×10^5 Pa. By combining the effects of the two main shocks, the net increase in the accumulated Cou-

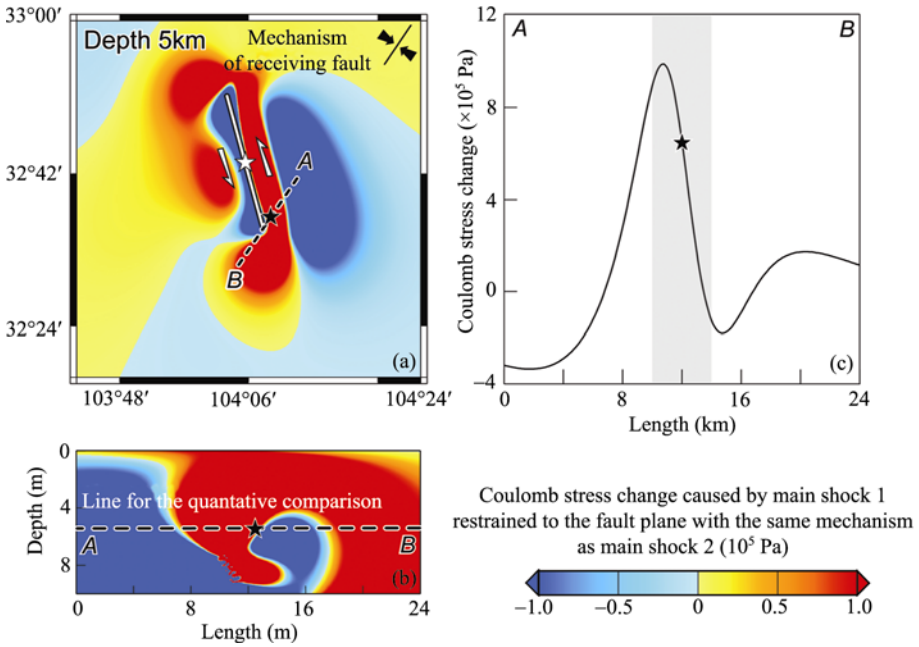

Figure 4 Coulomb stress change caused by the first main shock to the mechanism of the second event. (a) Coulomb stress change caused by the first main shock at a horizontal plan at the depth of the second earthquake (5 km). The Coulomb stress was increased at the location of the second event. (b) Coulomb stress change caused by the first main shock at the second fault plane. The hypocenter of the second main shock (marked as the black pentacle) is in the region of a stress increase. (c) Coulomb stress change on the second fault plane at 5-km depth. The Coulomb stress at the hypocenter of the second main shock (shown as the black pentacle) was increased by 6×10^5 Pa. The gray region marks the error in the location of the second event.

lomb stress change at the location of the third event is quite small (about 0.1×10^5 Pa). The triggering effect of the third event by these previous two main shocks is not obvious. Our calculations show that the first main shock had restrained the third event. However, the second main shock encouraged the occurrence of the third main shock.

4 Discussion

As shown in Figure 3 most aftershocks had occurred in the region where Coulomb stress had been increased. After the first main shock, the Coulomb stress had been increased significantly in the North-East region, which includes most of the aftershocks (Figure 3(a)). However, fewer aftershocks occurred in the west region where Coulomb stress had been decreased. Figure 3(b) shows that most aftershocks following the 1976 Songpan earthquake sequence took place within a narrow region along the faults. The spacial variation in the Coulomb stress change is shown at 5 km depth since the aftershocks were concentrated at 5 km depth[6].

The Coulomb stress at the location of the second main shock was increased by about 5×10^5 Pa after the first main shock. It is generally believed that when the Coulombs stress was increased by about 1×10^5 Pa at a nearby fault, an earthquake could be triggered[10]. Furthermore, the area of the location error (2 km) of the second main shock is also included in the region where the Coulomb stress was increased (Figure 4(c)) and therefore, it is likely that the first main shock had triggered the second one.

Compared with the triggering relationship between the first two shocks, the triggering relationship between the first two shocks and the third one is less obvious. The first shock had decreased the Coulomb stress at the location of the third shock (the third shock was restrained), but the second shock had increased the Coulomb stress at the third shock. The combination of the two shocks gives an increase of more than 0.1×10^5 Pa in the Coulomb stress change at the location of the third shock. Wan Yongge et al.[12] had suggested that the increase of Coulomb stress by $(0.1-1)\times10^5$ Pa is possible to trigger an earthquake. If that is the case, our analysis could explain why the third main shock was followed closely to the second event.

Our model calculations show a possible triggering relationship between left-lateral slip fault and thrust fault in the 1976 Songpan earthquake sequence. To further elaborate on this point, we calculated the Coulomb stress

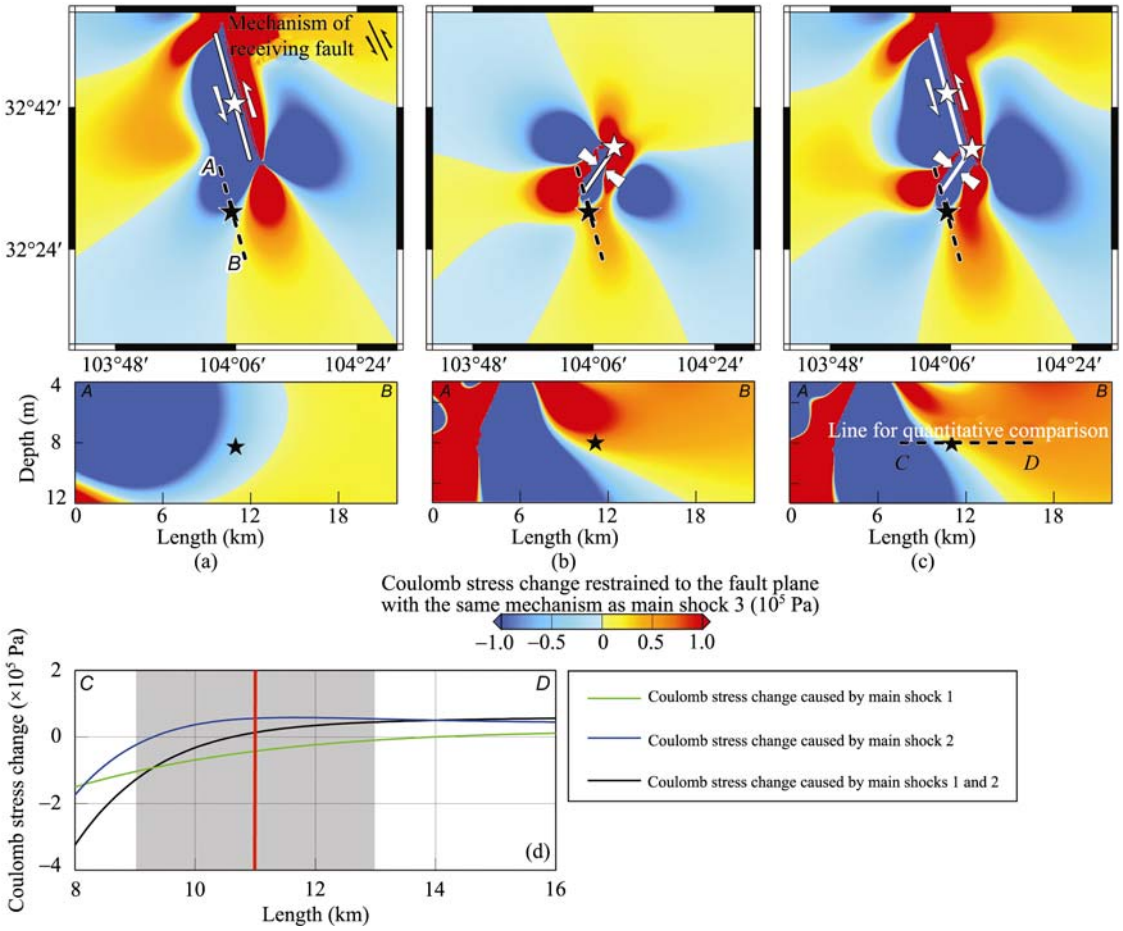

Figure 5 Coulomb stress changes on the location of the third event. (a) Coulomb stress change caused by the first main shock at the 8-km depth of the hypocenter of the third event (top) and on the third fault plane (bottom). Coulomb stress at the hypocenter of the third earthquake (black pentacle) was decreased. (b) Coulomb stress change caused by the second main shock at the 8-km depth of the hypocenter of the third event (top) and on the third fault plane (bottom). Coulomb stress at the hypocenter of the third earthquake (black pentacle) was increased. (c) Coulomb stress change caused by the combination of the first and second main shocks at the 8-km depth of the hypocenter of the third event (top) and on the third fault plane (bottom). The Coulomb stress change at the hypocenter of the third earthquake (black pentacle) was increased. (d) Coulomb stress change at 8-km depth on the third fault plane (red line marks the location of the third earthquake and the gray region shows the location error). The first main shock had decreased the Coulomb stress at the hypocenter of the third event by about 0.43×10^5 Pa and however, the second main shock had increased the Coulomb stress at the location by about 0.56×10^5 Pa. The net Coulomb stress change at the hypocenter of the third event was 0.13×10^5 Pa.

with different parameters for a fault system of a left-lateral slip fault and a thrust fault; each fault is 10 km long, 5 km wide (Figure 6).

The Coulomb stress change of an earthquake at a left-lateral slip fault is shown in Figure 6(a). It can be divided into four lobes: at one side of the left-lateral slip fault, the Coulomb stress increased in the forward direction of the fault slip and decreased in the opposite direction. We can call this a right-step form triggering, that is, if you stand in the forward direction of the source fault and make a right step, you will stand in the triggering region (where the Coulomb stress is increased). For comparison, as shown in Figure 6(c), the triggering relationship between a thrust fault as a source and a left-lateral slip fault as a receiving fault has a left-step triggering form.

On the other hand, for a case that both the source fault and the receiving fault are a left-lateral slip fault, most of the region is associated with a decrease in the Coulomb stress, suggesting a restrained relationship between left-lateral slip faults. Finally, as shown in Figure 6(d), an earthquake at a thrust fault can restrain a parallel thrust fault in most of the region except the adjacent area near the source.

We can conclude from these model calculations shown in Figure 6 that two adjacent parallel left-lateral slip faults such as the first and third main shocks of the 1976 Songpan earthquake sequence can hardly trigger

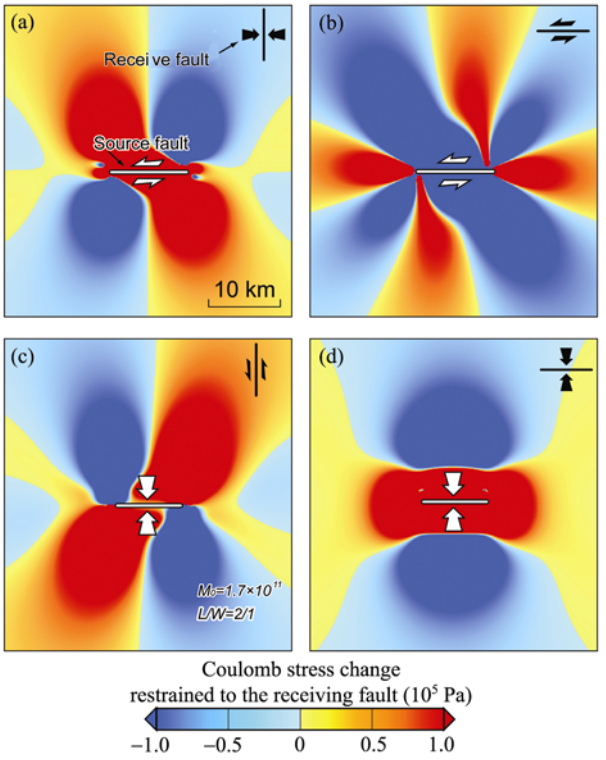

Figure 6 Coulomb stress change for different combination of faults. The thick while line marks the source fault, and the white arrows indicate the focal mechanism. The black line and the black arrows represent the orientation of the receiving fault and its mechanism, respectively.

each other while a thrust fault between these faults can facilitate the rupture continuity between these faults.

5 Conclusions

(1) Calculations of the coseismic Coulomb stress change suggested a good triggering relationship of the aftershocks by the main shocks.

(2) In the 1976 Songpan earthquake sequence, the first main shock at the northern segment of the Huya fault had likely triggered the second main shock located in the middle of the segment. The triggering effect of the third main shock is less obvious but it is possible that the third main shock was triggered by the two previous main shocks.

(3) Adjacent parallel left-lateral slip faults usually do not trigger each other. A thrust fault located between these faults can facilitate the transfer of the earthquakes between these left-lateral slip faults as seen for the case of the 1976 Songpan earthquake sequence.

We would like to thank Shinji Toda at Geological Survey of Japan, Ross Stein at U.S. Geological Survey and Jian Lin at Woods Hole Oceanographic Institution for their "Coulomb" program used in our calculations. Comments from two anonymous reviewers helped to improve the manuscript. We would also like to thank the editor invaluable advice.

1 Earthquake Administration of Sichuan Province.The 1976 Songpan Earthquake (in Chinese). Beijing: Seismic Press, 1979
2 Chen S F, Wilson C J L, Deng Q D, et al. Active faulting and block movement associated with large earthquakes in the Min Shan and Longmen Mountains, northeastern Tibetan Plateau. J Geophys Res, 1994, 99: 24025－24038
3 Wen X Z, Bai X L. Crust rupture graph and seismic tectonic of the North-west segment of Xianshuihe fault zone. Thesis Collection of Seismic Academic Conference about Xianshuihe Rupture Zone (in Chinese). Beijing: Seismic Press, 1985. 33－40
4 Allen C R, Luo Z L, Qian H, et al. Field study of a highly active fault zone: The Xianshuihe fault of southwestern China. Bull Geol Soc Am, 1991, 103: 1178－1199
5 Liu G P, Fu Z X. The Triggering Mechanism of the Largest Aftershock (Ms = 6.3) of the 1973 Luhuo Great Earthquake (Ms = 7.6). Earthquake Res Chin (in Chinese), 2002, 18(2): 175－182
6 Jones L M, Han W B, Hauksson E, et al. Focal mechanism and aftershock locations of the Songpan earthquake of August 1976 in Sichuan China. J Geophys Res, 1984, 89(B9): 7697－7707
7 Cheng E L et al. On the direction of the maximum compressive principal stress before and after the 1976 Songpan-Pingwu Earthquake (M=7.2) of Sichuan Province. Acta Seismal Sin (in Chinese), 1982, 4: 136－148
8 Diao G L, Cheng W Z, Li G F, et al. The focal mechanisms of small events of the 1976 Songpan earthquake sequence. Seismol Geomag Obs Res (in Chinese), 1996, 17: 34－41
9 Okada Y. Internal deformation due to shear and tensile faults in a half-space. Bull Seismol Soc Am, 1992, 82(2): 1018－1040
10 Toda S, Stein R S. Response of the San Andreas fault to the 1983 Coalinga-Nuñez Earthquake: An application of interaction-based probabilities for Parkfield. J Geophys Res, 2002, 107(B4): 11029－11044
11 King G C P, Stein R S, Lin J. Static stress changes and the triggering of earthquakes. Bull Seismal Soc Am, 1994, 84: 935－953
12 Wan Y G, Wu Z L, et al. "Stress Triggering" between different rupture events in several earthquakes. Acta Seismol Sin, 2000, 22: 568－576